

# Ionomer Composites Based on Sepiolite/Hydrogenated Poly(styrene butadiene) Block Copolymer Systems

Jose Luis Acosta, Luis González, Maria Carmen Ojeda, Carmen Del Río

*Instituto de Ciencia y Tecnología de Polímeros (Consejo Superior de Investigaciones Científicas), Juan de la Cierva 3, 28006 Madrid, Spain*

Received 25 June 2001; accepted 15 February 2002

**ABSTRACT:** Ionomeric composites based on sepiolite and hydrogenated poly(styrene butadiene) block copolymer were obtained and characterized from a microstructural and electrical point of view. Before blending, because of the high silanol group concentration in the sepiolite, the latter could be organophilized with suitable coupling agents. The resulting materials were easily processed into thin films or membranes 0.2–0.4 mm thick, their conductivity in some cases

approaching  $10^{-1}$  S/cm. Their suitability for film formation and good electrical properties indicate potential applications as electrolytes in polymer fuel cells. © 2002 Wiley Periodicals, Inc. *J Appl Polym Sci* 86: 3512–3519, 2002

**Key words:** differential scanning calorimetry (DSC); sepiolite; HSBR; ionomer composites

## INTRODUCTION

Sepiolite is a magnesium hydrosilicate with a microfibrillar morphology that is structured in discontinuous octahedral layers, which form open channels in the fiber direction.<sup>1,2</sup> This generates a microporous structure with a large surface area, to which water or other sorbables with suitable dimensions have access without causing structural swelling. Figure 1 shows a sample of a sepiolite structure with channels aligned in the fiber direction.

An important structural characteristic of this mineral is its surface structure, which is covered with silanol groups spaced every 5 Å along the fiber edges;<sup>3</sup> this may explain the material property-enhancing effects exerted by sepiolite in blends. The surface position makes the silanols easily accessible for coupling reactions, thereby increasing their polymer affinity, which, last but not least, improves the mechanical properties of the end product.<sup>4–6</sup> In a previous article,<sup>5</sup> it was reported that sepiolite, particularly when treated with silane coupling agents, reached reinforcement levels even higher than those of amorphous silica.

Exploiting the excellent reinforcing properties of sepiolite, as well as the presence of large numbers of silanol groups in its crystalline structure, we report on the synthesis and characterization of new ionomer composites that possess high proton conductivity and that, adequately designed, can be used as solid elec-

trolytes in polymer fuel cells for mobile telephony and automotive applications. In the pursuit of these aims, our first step consisted of sepiolite organophilization with suitable coupling agents, followed by the incorporation of the reaction product into a polymer thermoplastic system with high thermochemical and dimensional stability. The composite materials so obtained and conveniently processed into thin films were then structurally and electrically characterized.

## EXPERIMENTAL

### Materials

The hydrogenated poly(styrene butadiene) block copolymer (HSBR) used was Calprene CH-6120 from Repsol (Spain); it contained 30 wt % styrene units. The sulfonating reagent was acetyl sulfate prepared by the reaction of acetic anhydride and concentrated sulfuric acid (96%). 1,2-Dichloroethane (DCE) was previously dried with molecular sieves. The sepiolite was a Tolsa (Spain) product marketed under the trade name Pansil2. Bis-[3-(triethoxilyl)-propyl] tetrasulfane (Si-69) was provided by Degussa (France).

### Homogeneous HSBR sulfonation procedure

For the preparation of acetyl sulfate, first acetic anhydride was cooled below  $-10^{\circ}\text{C}$ , with a respective volume of 96% sulfuric acid being added. The solution was stirred, and DCE was added. The product obtained was maintained at  $0^{\circ}\text{C}$  in an ice bath until its addition to the reaction medium.

The HSBR sulfonation reaction was carried out according to the procedure described by Makowski et

Correspondence to: J. L. Acosta.

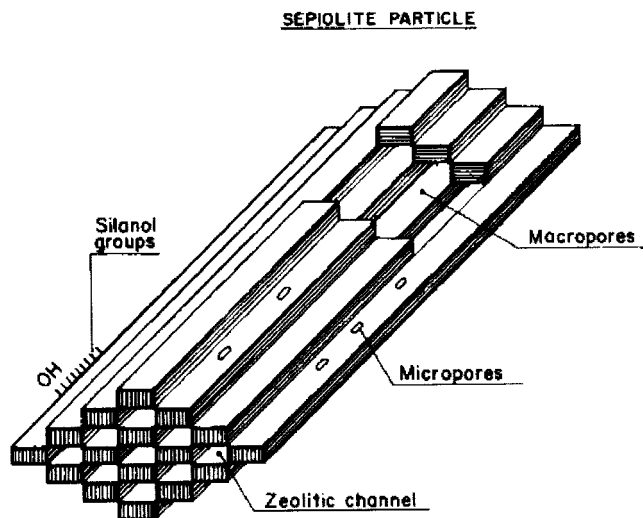


Figure 1 Schematic structure of a sepiolite crystal.

al.<sup>7,8</sup> The polymer was dissolved in DCE in a reactor and under constant stirring at 52–56°C. Then, it was purged with nitrogen. The addition of acetyl sulfate, prepared as previously described, ensued. For the entire duration of the sulfonation reaction, the solution was continuously stirred and purged with nitrogen. Samples were removed at the desired reaction times and precipitated in methanol or deionized water (1

L/10 g of polymer). The highly sulfonated polymer was partially soluble in methanol or water. It was then recovered by steam stripping and vacuum-dried at 50–60°C for a few days.

The complete removal of residual acid from the composite after sulfonation is important because the acid can interfere with the properties of the end product. The dried polymer was cut into small pieces and washed once with boiling deionized water and repeatedly with cold water until a neutral pH of the sewage was obtained. It was eventually vacuum-dried at 50–60°C and was then ready for testing.

The titration of the polymer against a standard potassium hydroxide solution (0.1N) with phenolphthalein as an indicator showed a sulfonation level greater than 15%.

### Sepiolite sulfonation procedure

First, the sepiolite was treated in a 0.5N hydrochloric acid (HCl) solution for 30 min under stirring, the mineral/solvent ratio being 90 g of sepiolite to 1 L of solution. Subsequently, the solid matter was filtered and washed several times with distilled water to a neutral reaction. The solid matter, when relatively dry, was dispersed in a methanol/water solution (90/10) under stirring with a Silverson instrument for 30 min,

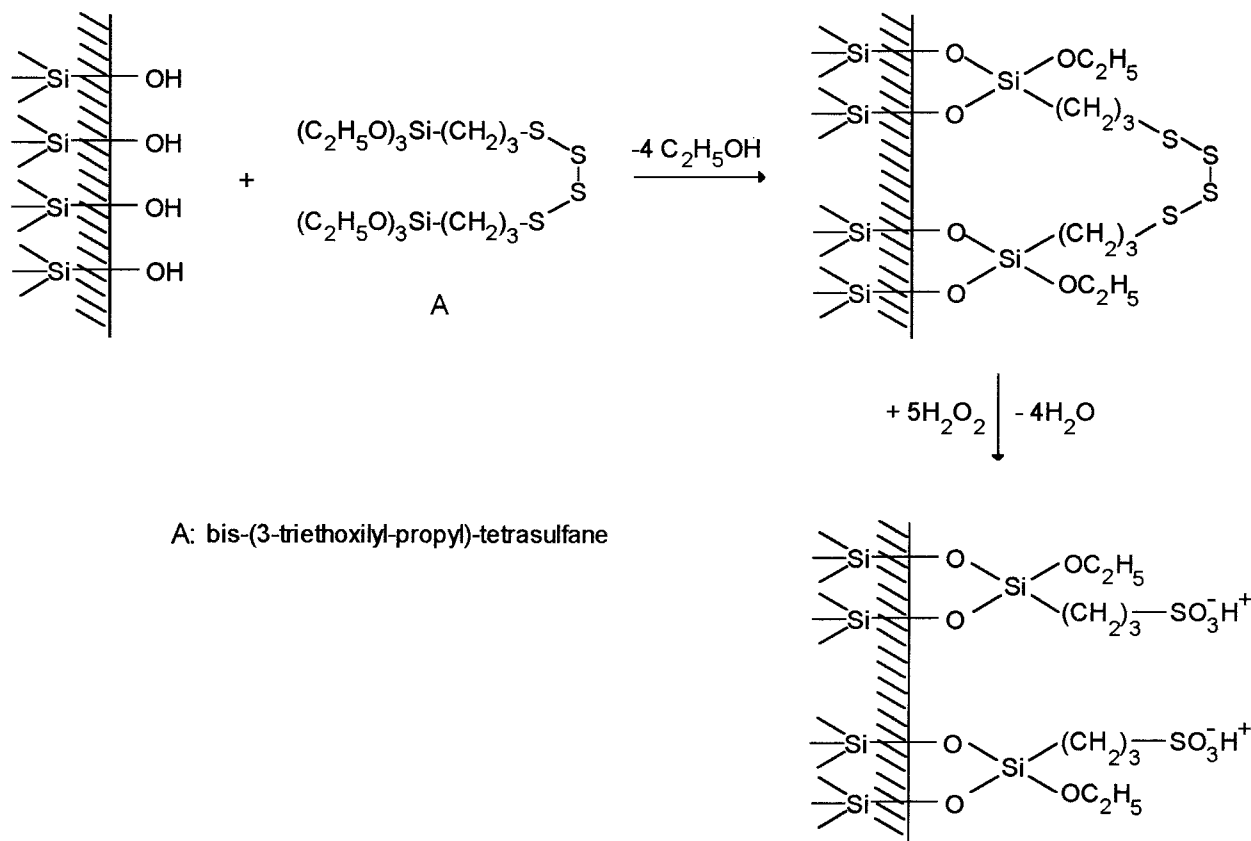


Figure 2 Scheme of the sulfonation reaction of sepiolite.

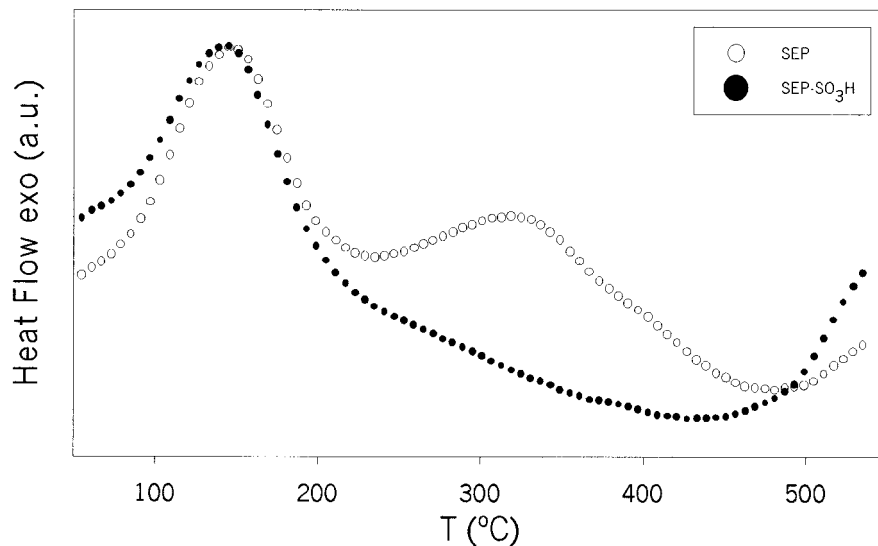


Figure 3 DSC thermograms of SEP and SEP-SO<sub>3</sub>H.

but the stirring was interrupted every 10 min so the sedimentation could be checked. Then, the dispersion was ultrasound-treated for final sedimentation checks. After these treatments, total desegregation of the sepiolite agglomerates was assumed to have been achieved.

At the same time, silane Si-69 was dissolved in methanol and then added under stirring to the sepiolite dispersion. The silane/sepiolite ratio was 0.2 g of silane to 1 g of sepiolite. Thirty minutes of stirring was considered to be enough for complete dispersion. Then, a 30/70 oxygenated water (H<sub>2</sub>O<sub>2</sub>)/methanol solution was added, the silane/H<sub>2</sub>O<sub>2</sub> ratio to be achieved being 1/5. The solution was left to react for 60 min. The solid was filtered and washed in methanol several times.

#### Blending procedure

An open two-roll mill was used to blend HSBR/sepiolite (SEP-1), HSBR/sepiolite-SO<sub>3</sub>H (SEP-2), and HSBR-SO<sub>3</sub>H/sepiolite-SO<sub>3</sub>H (SEP-3). A conventional mixing procedure was used at ambient temperature, the blending time being 20 min for maximized intermixing of the polymers.

#### Heterogeneous sulfonation procedure

The samples SEP-1 and SEP-2 were immersed in 0.2M chlorosulfonic acid in a 1,2-dichloroethane solution for various sulfonation times (3, 6, 9, and 24 h). The respective samples were superficially dried and washed, first in acetone and then in deionized Milli-Q water, and were allowed to dry for 8 h.

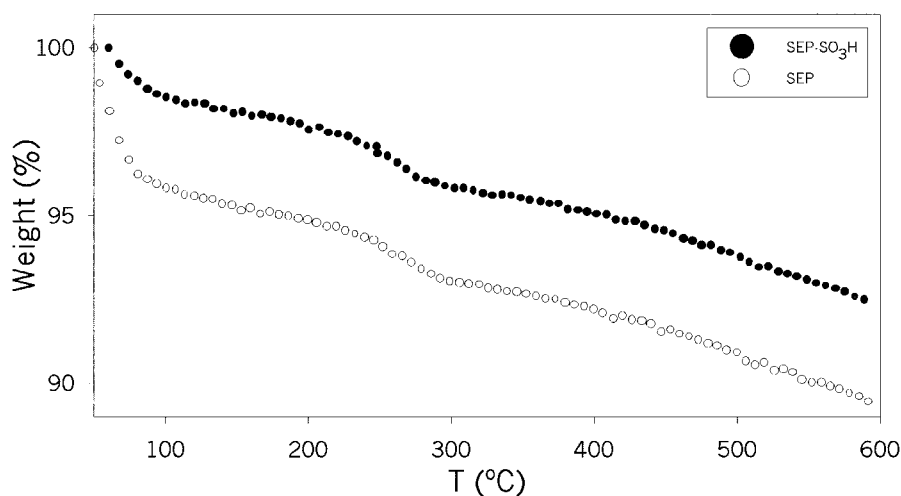


Figure 4 TGA curves of SEP and SEP-SO<sub>3</sub>H.

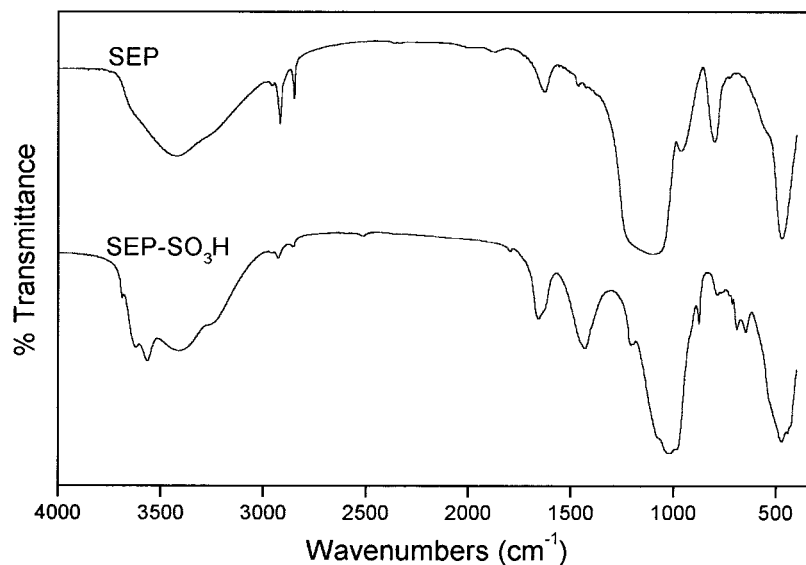
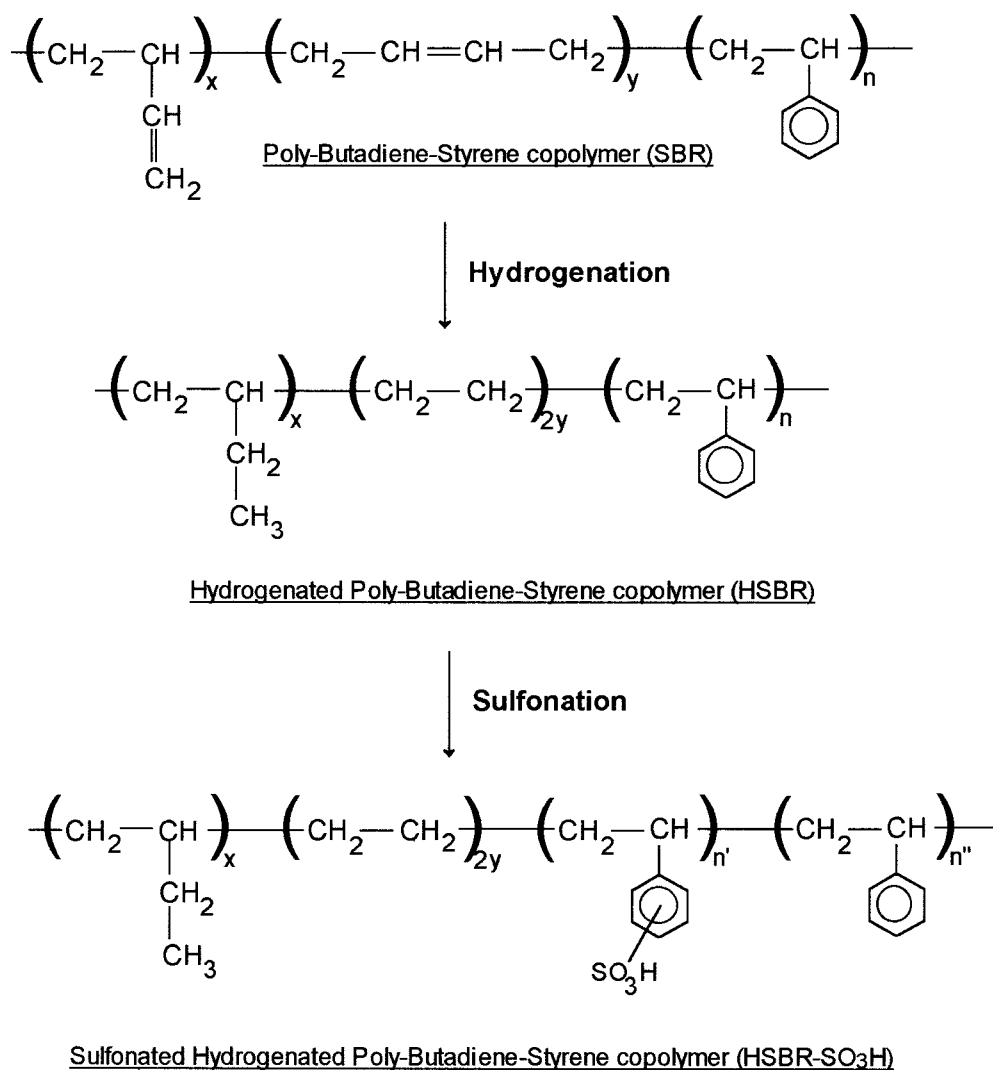

 Figure 5 FTIR spectra of SEP and SEP-SO<sub>3</sub>H.


Figure 6 Chemical mechanisms of the sulfonation reaction of HSBR.

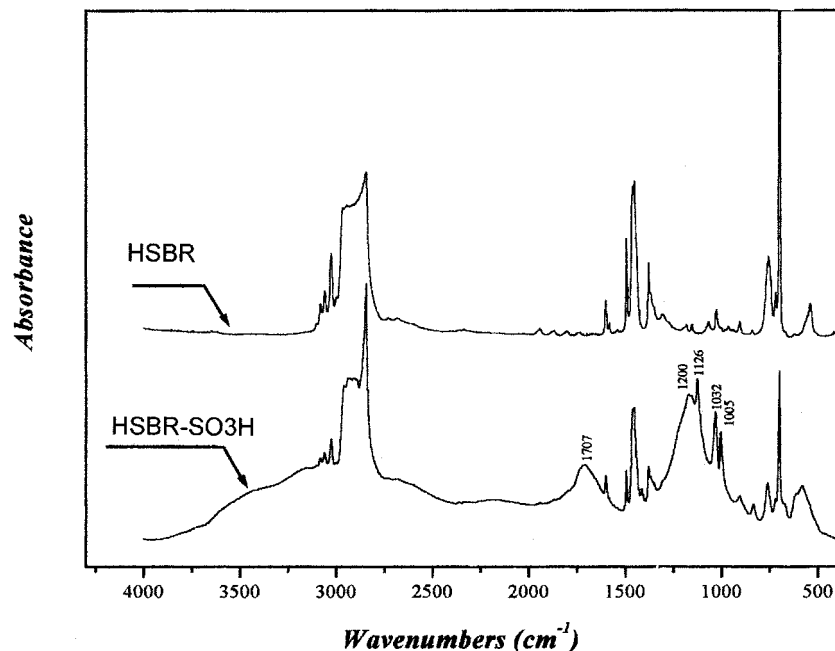


Figure 7 FTIR spectra of HSBR and HSBR-SO<sub>3</sub>H.

## Analyses

Thermogravimetric analysis (TGA) was performed with a PerkinElmer TGA7 from 50 to 550°C at a heating rate of 10°C/min.

A Nicolet 520 Fourier transform infrared (FTIR) spectrometer was used to record the infrared spectra of sepiolite and HSBR before and after sulfonation. A resolution setting of 4 cm<sup>-1</sup> and 32 scans were used. Samples were KBr pellets.

A Mettler 4000 differential scanning calorimeter was used for the thermal analysis of the different samples. The temperature range was -100 to 250°C for the polymer composites and 60 to 540°C for the sepiolite samples. Thermograms were recorded before and after sulfonation. The heating rate was 10°C/min for all the samples.

Dynamic mechanical analysis (DMA) measurements were performed with a Metravib RA C815A viscoanalyzer. Specimens were compression-molded in a Collin press at 130°C and 200 bars, and thin films were obtained with a thickness of 0.2–0.4 mm. They were analyzed in the compression mode at a deformation frequency of 5 Hz from -100 to 200°C.

Complex impedance spectroscopy was carried out with a Hewlett-Packard 4192A impedance analyzer at room temperature. The frequency range was 0.01–10,000 kHz.

## RESULTS AND DISCUSSION

### Sulfonated sepiolite: characterization

Both the pure (SEP) and sulfonated sepiolites (SEP-SO<sub>3</sub>H) were characterized with differential scanning

calorimetry (DSC), TGA, and FTIR spectroscopy. The sepiolite sulfonation reaction occurs according to the scheme indicated in Figure 2 when the procedure described in the Experimental section is applied.

Figure 3 shows the DSC thermograms obtained for SEP and SEP-SO<sub>3</sub>H, with notable differences between the untreated and the sulfonated samples. For both samples, a broad transition is found between approximately 75 and 200°C, marking the elimination of absorbed water from the material. With further heating, SEP shows another transition around 300°C, corresponding to the elimination of crystallized water. This latter transition does not appear in SEP-SO<sub>3</sub>H, confirming sepiolite sulfonation in good agreement with the scheme proposed in Figure 2.

Figure 4 shows TGA curves for SEP and SEP-SO<sub>3</sub>H. For both samples, a loss of water (absorbed and crystallized) takes place over the entire temperature range. However, the weight loss is higher for SEP (≈4%) than for SEP-SO<sub>3</sub>H (≈1.5%). These results indicate a change in the properties: crystallization water absorption is avoided and sepiolite sulfonation is confirmed.

The FTIR spectra (Fig. 5) of natural and modified sepiolite show  $\nu$  (O—H) stretching vibrations of the functional Si—OH groups present on the mineral surface, as well as those of the coordinated water molecules and zeolites in the region between 3700 and 3200 cm<sup>-1</sup>. For natural sepiolite, the latter are not visualized because of the presence of physically absorbed H<sub>2</sub>O, thereby forming hydrogen bridges with the Si—OH surface groups. The bands at 1655 and 1635 cm<sup>-1</sup> are assigned to zeolitic and coordinated water deformation vibrations. The region between 900 and 1100 cm<sup>-1</sup> is assigned to  $\nu$  (Si—O) stretching vibration

TABLE I  
DSC and DMA Transition Temperatures

Sample	COMPOSITION				DSC			DMA		
	HSBR wt %	HSBR-SO <sub>3</sub> H wt %	SEP wt %	SEP-SO <sub>3</sub> H wt %	T <sub>1</sub> (°C)	T <sub>2</sub> (°C)	T <sub>3</sub> (°C)	T <sub>1</sub> (°C)	T <sub>2</sub> (°C)	T <sub>3</sub> (°C)
SEP-1	70	—	30	—	-41.9	171.1	—	-43.0	113.5	—
SEP-2	70	—	—	30	-41.8	169.1	206.5	-43.5	112.1	181.0
SEP-3	—	70	—	30	-41.8	163.6	—	-44.0	137.5	—

bands. The surface-treated sepiolite spectrum shows significant differences in comparison with that of the untreated sample. The zone between 3700 and 3200  $\text{cm}^{-1}$  shows clearly differentiated bands that were masked by the presence of physically absorbed water in the untreated sample but now become visible because of sulfonation. The intense band at 1400  $\text{cm}^{-1}$  is attributed to a sulfonic group stretching vibration.

#### Sulfonated HSBR: characterization

As indicated in the Experimental section, HSBR was likewise sulfonated and characterized. The reaction develops according to the scheme reproduced in Figure 6. FTIR was used to confirm the sulfonation of the styrene groups in the HSBR polymer. Figure 7 compares a series of FTIR spectra before and after sulfonation. The changes in the combination vibrations (finger bands) between 1950 and 1650  $\text{cm}^{-1}$  cannot be overlooked and are particularly characteristic of the phenyl group. The band centered at 1200  $\text{cm}^{-1}$  is characteristic of the O=S=O asymmetric stretching vibration. Absorbencies at 1005 and 1126  $\text{cm}^{-1}$  result

from the vibrations of the phenyl ring with substitutions by a sulfonated group and a sulfonated anion attached to the phenyl ring, respectively.

#### Microstructural analysis of the membranes

A microstructural analysis of the experimental films was based on DSC and DMA. Table I and Figure 8 show the transitions observed with DSC. The transition occurring at the lower temperature ( $T_1$ ) corresponds to the glass-transition temperature of the hydrogenated polybutadiene ( $T_g^{\text{HPB}}$ ), defined as the inflexion point of the transition. It appears unaltered in all the samples and is, therefore, indicative of the fact that sulfonic group incorporation does not affect  $T_g^{\text{HPB}}$ .

At higher temperatures, there appear certain endothermal transitions ( $T_2$  and  $T_3$ ). In the absence of sulfonated sepiolite (SEP-1), there appears only a single transition at 171°C that is assigned to the inorganic filler. For the sample containing sulfonated sepiolite

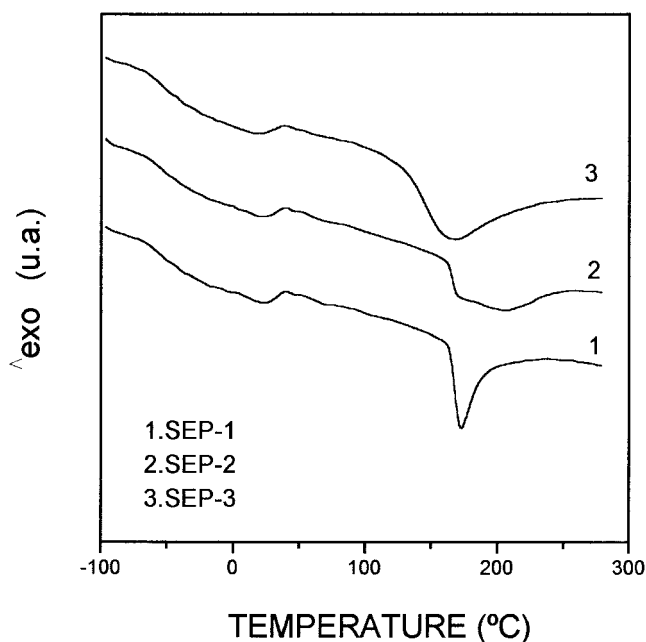


Figure 8 DSC thermograms of the different samples.

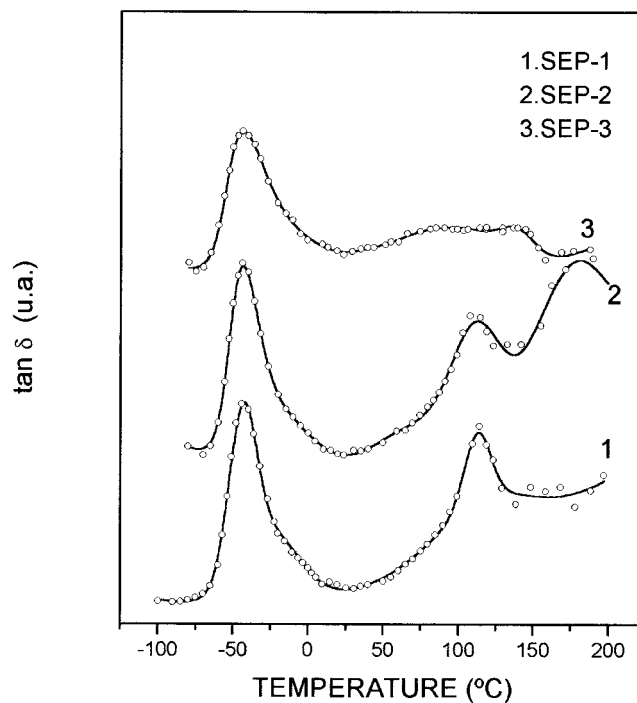


Figure 9 DMA relaxation spectra of the different samples.

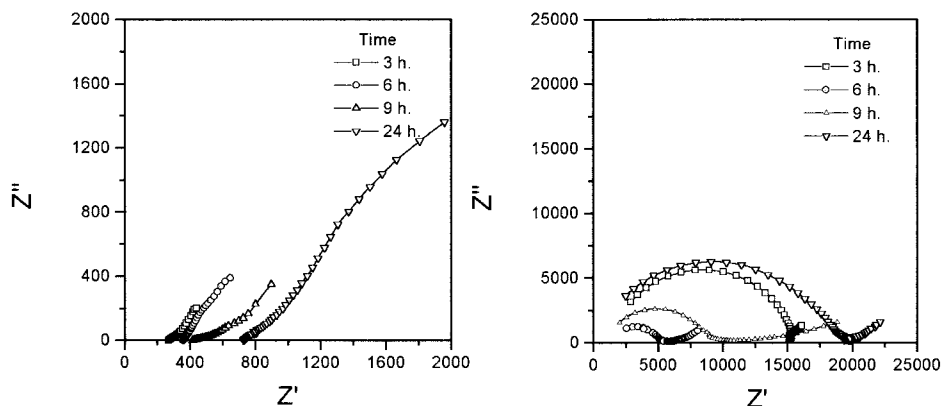


Figure 10 Impedance plots at different sulfonation times for SEP-1 and SEP-2.

(SEP-2), this transition drops slightly, becomes wider, and actually branches into two transitions, the second one (206.5°C) being related to the cluster phase resulting from the advent of ionic groups triggered by electrostatic forces. When the sulfonated sepiolite is incorporated into a polymeric HSBR-SO<sub>3</sub>H matrix (SEP-3), the content of ionic groups increases, and this latter transition is not visible in the temperature range used.

DMA yields relatively comparable results. Table I compiles the relaxation temperatures observed, whereas Figure 9 shows the dynamic mechanical spectra of the three samples. The first relaxation ( $T_1$ ) to be observed relates to  $T_g^{\text{HPB}}$ , which does not vary when the unsulfonated polymer is blended with either sulfonated or natural sepiolite, nor does it vary for the respective blends with the sulfonated polymer, as observed for DSC analysis.

At higher temperatures, there appears a second relaxation  $T_2$  (and, in one case, even a third  $T_3$ ) that corresponds to the glass-transition temperature of the polystyrene component ( $T_g^{\text{PS}}$ ), a transition that DSC is unable to detect. This relaxation increases by 24°C for SEP-3, that is, the sample consisting of a sulfonated matrix and a sulfonated filler (HSBR-SO<sub>3</sub>H + SEP-SO<sub>3</sub>H = SEP-3), because of the increment in the ion

content in the system. Sulfonic group incorporation into the system restricts the segmental movements of the styrene block in the copolymer. In one of the samples (SEP-2) and at a considerably higher temperature (181°C), a third relaxation is observed that does not present for the other two samples. This last relaxation, similar to what was observed in DSC analysis, is assigned to the presence of clusters in the composite as a result of the ionic aggregates.

#### Electrical analysis of the membranes

Ion conductivity was measured with complex impedance spectroscopy for the three samples, and consistently low values (ca.  $10^{-9}$  S/cm<sup>-1</sup>) were obtained that were characteristic of insulating materials.

For the purpose of improving these results, the kinetics of heterogeneous sulfonation were determined for samples SEP-1 and SEP-2, with their ionic conductivity measured at different sulfonation times. Figure 10 shows complex impedance diagrams for different sulfonation times. The conductivity results obtained are compiled in Table II. Several findings ought to be highlighted. First, heterogeneous sulfonation is effective at short sulfonation times; that is, conductivity

TABLE II  
Sulfonation Kinetics of the Samples and Conductivity Analysis

Sample	COMPOSITION			Sulfonation time (h)	Conductivity (S cm <sup>-1</sup> )
	HSBR wt %	SEP wt %	SEP-SO <sub>3</sub> H wt %		
SEP-1	70	30	—	0	>10 <sup>-9</sup>
				3	1.81 × 10 <sup>-2</sup>
				6	1.41 × 10 <sup>-2</sup>
				9	1.50 × 10 <sup>-2</sup>
				24	4.33 × 10 <sup>-3</sup>
SEP-2	70	—	30	0	>10 <sup>-9</sup>
				3	6.94 × 10 <sup>-5</sup>
				6	2.22 × 10 <sup>-4</sup>
				9	1.21 × 10 <sup>-4</sup>
				24	5.07 × 10 <sup>-5</sup>

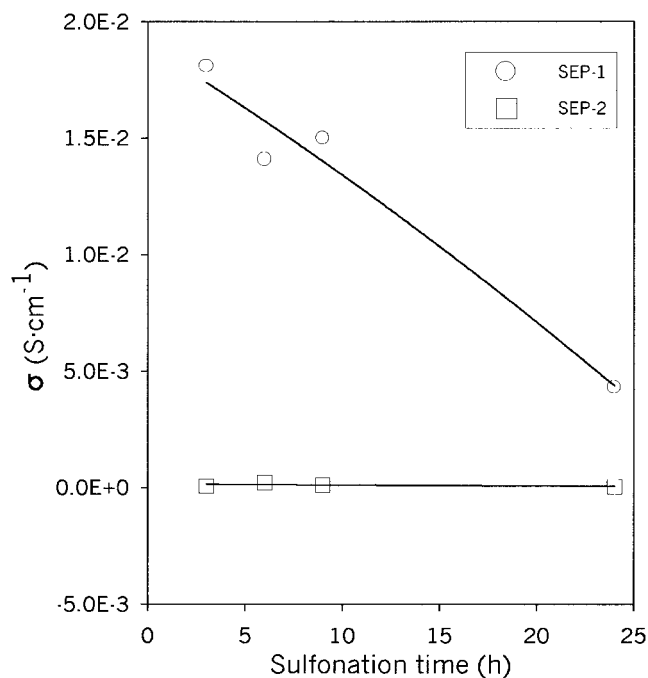


**Figure 11** Ionic conductivity as a function of the sulfonation time for SEP-1 and SEP-2.

improves up to 7 orders of magnitude with 3 h of sulfonation. Second, the highest values are obtained for sample SEP-1, that is, the sample that initially does not contain sulfonic groups in the sepiolite. Finally, at the longest sulfonation time (24 h), conductivity does not only not improve but, on the contrary, diminishes remarkably (Fig. 11). This loss in conductivity goes hand in hand with a considerable deterioration of the samples themselves.

## References

1. Nagy, B.; Bradley, W. F. *Am Miner* 1955, 40, 885.
2. Brauner, K.; Presinger, A. A. *Miner Pet Mitt* 1956, 6, 120.
3. Serna, J.A. Ph.D. Thesis, Universidad Complutense de Madrid, 1973.
4. González, L.; Ibarra, L.; Rodríguez, A. *Angew Makromol Chem* 1982, 104, 189.
5. González, L.; Ibarra, L.; Royo, J.; Rodríguez, A.; Chamorro, C. *Kautsch Gummi Kunstst* 1987, 40, 1053.
6. González, L.; Ibarra, L.; Chamorro, C. *Rubber Chem Technol* 1987, 60, 606.
7. Makowski, H. S.; et al. U.S. Pat. 3,870,841 (1975).
8. Makowski, H. S.; et al. U.S. Pat. 4,184,988 (1980).